MIT Open Access Articles

An EMG-based robot control scheme robust to time-varying EMG signal

An EMG-Based Robot Control Scheme Robust to Time-Varying EMG Signal Features

Panagiotis K. Artemiadis, *Member, IEEE*, and Kostas J. Kyriakopoulos, *Member, IEEE*

Abstract—Human–robot control interfaces have received increased attention during the past decades. With the introduction of robots in everyday life, especially in providing services to people with special needs (i.e., elderly, people with impairments, or people with disabilities), there is a strong necessity for simple and natural control interfaces. In this paper, electromyographic (EMG) signals from muscles of the human upper limb are used as the control interface between the user and a robot arm. EMG signals are recorded using surface EMG electrodes placed on the user's skin, making the user's upper limb free of bulky interface sensors or machinery usually found in conventional human-controlled systems. The proposed interface allows the user to control in real time an anthropomorphic robot arm in 3-D space, using upper limb motion estimates based only on EMG recordings. Moreover, the proposed interface is robust to EMG changes with respect to time, mainly caused by muscle fatigue or adjustments of contraction level. The efficiency of the method is assessed through real-time experiments, including random arm motions in the 3-D space with variable hand speed profiles.

Index Terms—Electromyographic (EMG) control, muscle fatigue, neurorobotics.

I. Introduction

ROBOTS came to light approximately 50 years ago. However, the way humans interface and control them is still an important issue. The human–robot interface plays an utmost significant role, especially if we realize that the use of robots is increasingly widening to everyday life tasks (e.g., service robots and robots for clinical applications). A large number of interfaces have been proposed in earlier studies [1]. Most of the previous work proposes complex mechanisms or systems of sensors, while in most cases, the user should be trained to map his/her action (i.e., 3-D motion of a joystick or a haptic device) to the motion desired for the robot. In this paper, a new means of control interface is proposed, in which the user performs natural motions with his/her upper limb. Surface electrodes recording the electromyographic (EMG) activity of the muscles of the upper limb are placed on the user's skin. The recorded muscle activity was transformed to kinematic variables that were used to control the robot arm. Since an anthropomorphic robot arm was used, the user did not have to be acquainted with the interface

mapping, since natural arm motions essentially sufficed to directly control the robot arm.

EMG signals have often been used as control interfaces for robotic devices. However, since the musculoskeletal system is very complex and the relationship of the EMG signals and arm motion is highly nonlinear [2], in most cases, only discrete control has been realized. Previous work focused, for example, only on the directional control of robotic wrists [3] or on the control of multifingered robot hands to a limited number of discrete postures [4]. Arm exoskeletons [5] have used EMG signals as control interface in the past. However, most of the previous works decode only finite arm or hand postures from EMG signals [6], although controlling a robot using only finite postures can cause many problems regarding smoothness of motion, especially in the cases where the robot performs everyday life tasks. Therefore, effectively interfacing a robot arm with a human entails the necessity for continuous and smooth control.

Continuous models have been built in the past in order to decode arm motion from EMG signals. The Hill-based muscle model [7], whose mathematical formulation can be found in [2], is most used in the literature [8], [9]. However, only a few DOFs were analyzed (i.e., 1 or 2), since the nonlinearity of the model equations and the large number of the unknown parameters for each muscle made the analysis rather difficult. Therefore, random arm motions were never efficiently decoded through EMG signals for the scope of the EMG-based robot control.

An important factor that is present in the EMG-based controlled robotic systems, though it has never been investigated until now, is the fact that EMG signals change with respect to time.[1] These changes can be caused by muscle fatigue, changes in the level of muscle force production, sweat at the recording site, or small electrode movement with respect to its initial position [10]. However, all the algorithms that have been proposed use stationary models for translating EMG signals into motion. Therefore, time variation of EMG signals is not incorporated, making the aforementioned methods applicable only for short time periods. The authors recently proposed a method for incorporating time-vayring EMG signal characteristics in decoding arm motion from muscle activations [11]. The present paper is a significant extension of the previous one, since a new signal feature (median frequency) is included in the analysis, which proves to capture most information about muscle fatigue [12]. Moreover, more subjects are used in this study, for multiple and long experimental sessions.

In this paper, we propose a methodology for controlling an anthropomorphic robot arm using surface recordings from the

---

[1]Explicit time variation is meant here, i.e., during a course of arm movements, the same motions could result in different EMG signals.

muscles of the upper limb, which is robust to time variation of EMG signals. The system architecture was divided into two phases: the training and the real-time operation. During the training phase, the user was instructed to move his/her arm in random patterns with variable speed in the 3-D space. A position tracking system was used to record the arm motion during reaching, while surface EMG electrodes were used to record the activity of nine muscles of the shoulder and the elbow. EMG signals and computed signal features are incorporated into a classification and estimation methodology in order to train a set of models that will be used in real time for arm motion estimation using only EMG recordings. As soon as the training phase had finished, the real-time-operation phase commenced. A control law that utilized the motion estimates was applied to the robot arm actuators. In this phase, the user could teleoperate the robot arm in real time, while he could correct any possible robot deviations since he had visual contact with the robot. The efficacy of the proposed method is assessed through a large number of experiments (four subjects, five sessions per subject, 3.5 min each) during which the users controlled the robot arm in performing random movements in the 3-D space.

II. METHODS

A. Data Acquisition and Processing

The motion of the upper limb was analyzed in 3-D space, though excluding the wrist joint for simplicity. Therefore, the shoulder and the elbow joints were of interest. Three rotational DOFs were used to model the shoulder joint and one rotational DOF for the elbow joint.

For the training of the proposed system, the motion of the upper limb should be recorded and joint trajectories should be extracted. Therefore, in order to record the motion, and then, extract the joint angles of the four modeled DOFs, a magnetic position tracking system was used. The system was equipped with two position trackers and a reference system, with respect to which the 3-D position of the trackers was provided. In order to compute the four joint angles, one position tracker was placed at the user's elbow joint (at the olecranon) and the other one at the wrist joint (at the styloid process of radius). The reference system was placed on the user's shoulder. The setup as well as the four modeled DOFs are shown in Fig. 1. Let $\mathbf{T_1} = \begin{bmatrix} x_1 & y_1 & z_1 \end{bmatrix}^T$ and $\mathbf{T_2} = \begin{bmatrix} x_2 & y_2 & z_2 \end{bmatrix}^T$ be the position of the trackers with respect to the tracker reference system. Let q_1, q_2, q_3, and q_4 be the four joint angles modeled as shown in Fig. 1. Finally, by solving the inverse kinematic equations, the joint angles are given by

$$q_1 = \arctan 2\left(\pm y_1, x_1\right)$$

$$q_2 = \arctan 2\left(\pm\sqrt{x_1^2 + y_1^2}, z_1\right)$$

$$q_3 = \arctan 2\left(\pm B_3, B_1\right)$$

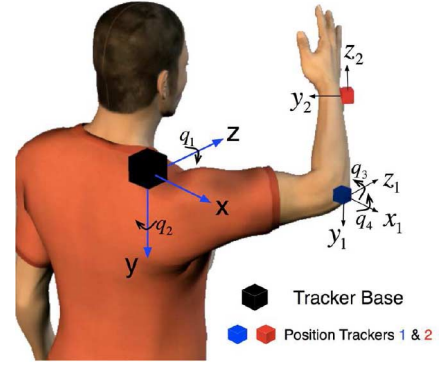$$q_4 = \arctan 2\left(\pm\sqrt{B_1^2 + B_3^2}, -B_2 - L_1\right) \quad (1)$$

Fig. 1. User moves his arm in the 3-D space. Two position tracker measurements are used for computing the four joint angles. The tracker base reference system is placed on the shoulder. The variables q_1 and q_2 jointly simulate the shoulder flexion–extension and adduction–abduction, q_3 corresponds to shoulder internal–external rotation, while q_4 corresponds to elbow flexion–extension.

where

$$B_1 = x_2 \cos\left(q_1\right)\cos\left(q_2\right) + y_2 \sin\left(q_1\right)\cos\left(q_2\right) - z_2 \sin\left(q_2\right)$$

$$B_2 = -x_2 \cos\left(q_1\right)\sin\left(q_2\right) - y_2 \sin\left(q_1\right)\sin\left(q_2\right) - z_2 \cos\left(q_2\right)$$

$$B_3 = -x_2 \sin\left(q_1\right) + y_2 \cos\left(q_1\right) \quad (2)$$

where L_1 is the length of the upper arm. The length of the upper arm was computed from the distance of the first position tracker from the base reference system. Likewise, the length of the forearm L_2 was computed from the distance between the two position trackers. Finally, one out of the multiple solutions given by (1) was selected for each joint angle at each time instance, based on the range of motion for each human joint; if this was not enough for solving the ambiguity, the solution selected was the one that was closer to the previously computed value.

The position tracking system provided the position vectors $\mathbf{T_1}$ and $\mathbf{T_2}$ at the frequency of 30 Hz. Using an antialiasing finite-impulse-response (FIR) filter, these measurements were resampled at the frequency of 1 kHz, in order to be consistent with the muscle activations sampling frequency.

Motion variability is important for such methods; therefore, during training, the user was instructed to move his/her arm to all the possible ranges of motion for the shoulder and elbow, at various speeds. The 3-D positions of the user's hand during this session, along with the distribution of the arm velocity, are shown in Fig. 2. As can be seen, the user was moving his/her hand in a large portion of the available workspace, with speed varying inside the range of arm speed profiles for everyday life tasks (i.e., 150–200°/s for most joints) [13]. The frequency spectrum of the hand velocity is also shown, in order to prove that the user was performing arm motions that spanned most of the usual frequency range of arm motions in everyday life tasks (i.e., 1–1.5 Hz) [13].

Regarding muscle recordings, a group of nine muscles, mainly responsible for the analyzed motion, was recorded: deltoid (anterior), deltoid (posterior), deltoid (middle), pectoralis major, pectoralis major (clavicular head), trapezius, biceps brachii, brachioradialis, and triceps brachii. Surface bipolar EMG electrodes, used for recording, were placed on the
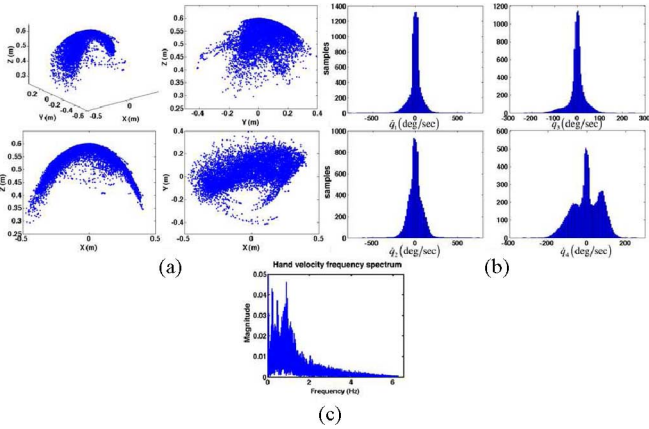
Fig. 2. User's upper limb motion during training. (a) 3-D position of the user's hand in the Cartesian system defined in Fig. 1, and its three 2-D views. (b) Distributions of the rotational velocities per joint during the training phase. (c) Frequency spectrum of the user's hand velocity during training.

user's skin following the directions given in [14]. The raw EMG recordings were preprocessed, i.e., full-wave-rectified, low-pass-filtered, and normalized to their maximum voluntary isometric contraction value [2].

B. Time Variation of EMG

It is widely reported in the biomechanics and physiology literature that EMG signals are not stationary, in the sense that some signal features change with respect to time. In other words, EMG recordings for the same motion change with respect to time. In this paper, we want to monitor these changes, and build a method capable of incorporating these signal changes into the motion decoding scheme. In this way, EMG changes will not affect the decoding accuracy. This will be done by defining a set of EMG classes, where each class will correspond to cases where the EMG recordings will have some specific characteristics. After analyzing the data recorded during the training period, we computed a set of signal features that were observed to vary with respect to time. It must be noted that the extraction of the signal features was done at the raw EMG recordings, before the preprocessing mentioned earlier (i.e., rectification, low-pass filtering, and normalization). These are listed as follows.

1) *Integral of absolute value (IAV)*: The IAV of the EMG signal of one muscle was calculated by $\text{IAV} = (1/M) \sum_{i=1}^{M} |e_i|$, where $|e_i|$ is the absolute value of the ith sample and M is the number of samples in each segment. Raw signal was digitized at the frequency of 1 kHz and partitioned in overlapping segments (i.e., time bins) of 100 ms. Therefore, $M = 100$; since the bins were overlapping, the signal characteristic was computed at the frequency similar to that of the acquisition (i.e., 1 kHz).

2) *Zero crossing (ZC)*: This was defined as the number of times the signal passed the zero-amplitude axis. It was calculated by $\text{ZC} = \sum_{i=1}^{M} \text{sgn}(-e_i e_{i+1})$, where

$$\text{sgn}(e) = \begin{cases} 1, & \text{if } e > 0 \\ 0, & \text{otherwise.} \end{cases} \quad (3)$$
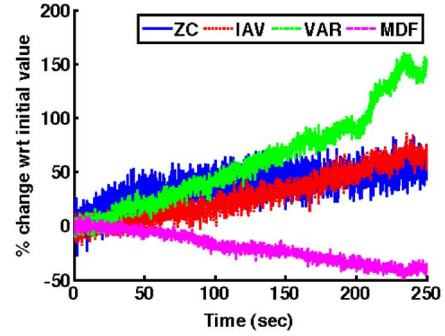

Fig. 3. Variation of the four selected EMG characteristics during a 4-min experiment. The percentage change with respect to their initial values is plotted for each characteristic. Based on their final values (at time $t = 250$ s), and starting from the top to the bottom of the figure, the curves correspond to (top) VAR, IAV, ZC, and (bottom) MDF.

3) *Variance (VAR)*: The variance was a measure of the signal power and was calculated by $\text{VAR} = (1/(M-1)) \sum_{i=1}^{M} e_i^2$.

4) *Median frequency (MDF)*: The median frequency is the frequency at which the power spectrum of the recorded signal is divided into two parts of equal power. It is mathematically described by $\int_0^{\text{MDF}} P(\omega)\, d\omega = \int_{\text{MDF}}^{\infty} P(\omega)\, d\omega = (1/2) \int_0^{\infty} P(\omega)\, d\omega$, where $P(\omega)$ is the power spectral density and ω is the frequency of the signal. In our case, the MDF was computed for $0 < \omega < 500$ Hz.

The calculation of the previously defined signal features for the training period showed that there was significant variation in their values with respect to the experiment time. Similar behavior was reported in previous studies [15]. The variation of these characteristics, for one muscle, with respect to their initial values (i.e., at the start of the training phase) is shown in Fig. 3. Similar behavior was noticed for all the recorded muscles.

From the earlier analysis, a feature vector **F** can be defined, including the four aforementioned signal characteristics that can be computed at each time bin for each muscle. However, EMG signals' features are not only time-dependent, but are also related with the performed motion. Therefore, the feature vector **F** should also include the motion variables of the arm. As motion variables, the angular velocities $\dot{q}_w, w = 1, \ldots, 4$, were used, since it was shown from the data recordings that their dependence on the EMG signal features was stronger than the dependence of the joint angles. The feature vector **F** of each muscle i, at each time instance m, was finally given by

$$\mathbf{F}_m^{(i)}$$
$$= [\text{IAV}_m^{(i)} \quad \text{ZC}_m^{(i)} \quad \text{VAR}_m^{(i)} \quad \text{MDF}_m^{(i)} \quad \dot{q}_{1m} \quad \dot{q}_{2m} \quad \dot{q}_{3m} \quad \dot{q}_{4m}],$$
$$i = 1, \ldots, 9, \qquad m = 1, \ldots \quad (4)$$

where time instance m and $m-1$ are 1 ms away and correspond to the time instances the signal features were computed.

The purpose of this paper, as described before, is to classify the recorded EMG signals, according to their time-varying features, in order to be able to switch between different models for EMG-based motion decoding. In other words, a class

$f^{(i)}$ for each muscle i should be defined, denoting a specific value *range* for the time-varying features, which is different among the classes. The set of these classes is defined as $\mathbf{f}^{(i)} = \{f_1^{(i)}, f_2^{(i)}, \ldots, f_n^{(i)}\}$, where n is the number of classes for the muscle i. In order to decide the class for the muscle i at each time instance m, according to the measured feature vector $\mathbf{F}_m^{(i)}$, we needed to compute the conditional probability of the muscle being at the class $f_{(j)}^{(i)}$, $j = 1, \ldots, n$, where n is the possible classes, given the feature vector $\mathbf{F}_m^{(i)}$, i.e., $P\left(f_{(j)}^{(i)} | \mathbf{F}_m^{(i)}\right)$. This was done using the Bayes theorem [16], which, in our case, is described by the following equation:

$$P\left(f_{(j)}^{(i)} | \mathbf{F}_m^{(i)}\right) = \frac{p\left(\mathbf{F}_m^{(i)} | f_{(j)}^{(i)}\right) P\left(f_{(j)}^{(i)}\right)}{p\left(\mathbf{F}_m^{(i)}\right)}, \qquad j = 1, \ldots, n \tag{5}$$

where $p(\mathbf{F}_m^{(i)} | f_{(j)}^{(i)})$ is the probability density function (pdf) of the feature vector $\mathbf{F}_m^{(i)}$ given the class $f_{(j)}^{(i)}$, $P(f_{(j)}^{(i)})$ the prior probability of the class being $f_{(j)}^{(i)}$, and

$$p\left(\mathbf{F}_m^{(i)}\right) = \sum_{j=1}^{n} p\left(\mathbf{F}_m^{(i)} | f_{(j)}^{(i)}\right) P\left(f_{(j)}^{(i)}\right). \tag{6}$$

It indicates the evidence factor that can be considered as a scale factor that guarantees the posterior probabilities sum to 1. The n classes for each muscle i were considered equally likely to happen, i.e., $P(f_{(1)}^{(i)}) = P(f_{(2)}^{(i)}) = \cdots = P(f_{(n)}^{(i)}) = 1/n$.

In order to decide the class of the muscle i at each time instance m, related to the recorded time-varying signal features, we used (5) to compute the probability of being at the class $f_{(j)}^{(i)}$ for each j, $j = 1, \ldots, n$, given the feature vector $\mathbf{F}_m^{(i)}$. Then, the class with the largest probability was assigned for muscle i. This was done at every time step m, using the new feature vector $\mathbf{F}_m^{(i)}$. However, the pdf of the feature vector $\mathbf{F}_m^{(i)}$ given the class $f_{(j)}^{(i)}$, $p(\mathbf{F}_m^{(i)} | f_{(j)}^{(i)})$, the so-called *likelihood* term, needed to be computed. This was achieved using the data collected through the training period. Since there was no specific relation between the coefficients of the feature vector, a flexible method of modeling was used, called finite mixture models [16]. In our case, where more than one components (i.e., features) were to be modeled, which were not independent, a multivariate mixture model was used. Moreover, a common assumption in practice is to take the component densities to be Gaussian. Therefore, a multivariate Gaussian mixture model (GMM) was used for modeling the multivariate density of the feature vector $\mathbf{F}_m^{(i)}$. Let $\mathbf{F}_m^{(i)}$ be the observed feature vector of muscle i at time instance m during the training procedure. The pdf of this was modeled using a GMM, which is defined by $p(\mathbf{F}_m^{(i)}) = \sum_{h=1}^{g} \pi_h \phi_h(\mathbf{F}_m^{(i)}, \mu_h, \Sigma_h)$, where $\phi_h(\mathbf{F}_m^{(i)}, \mu_h, \Sigma_h)$ represents a multivariate Gaussian density function, with $\mu_\mathbf{h}$ being the mean vector and Σ_h the respective covariance matrix, and $\pi = [\pi_1 \cdots \pi_g]^T$ is the vector of mixing proportions of the mixture, which sums to 1. Using the collected training data, the parameters of the GMM, i.e., π, μ, and Σ, were fitted using

the expectation–minimization (EM) algorithm [16]. The number of the Gaussian components g was determined by using the Akaike criterion, which is a widely used measure of goodness of fit of an estimated statistical model.

In our case, the mixture components could be used for clustering the signal characteristics into the aforementioned classes. This could be done once the mixture models has been fitted using a probabilistic clustering of the data into g clusters that could be obtained in terms of the fitted posterior probabilities of component membership for the data. An outright assignment of the data into g clusters was achieved by assigning each data point to the component to which it has the highest posterior probability of belonging. For this purpose, we define $r(\mathbf{F}_m^{(i)})$ as an allocation rule for assigning the feature vector $\mathbf{F}_m^{(i)}$ to one of the components of the mixture model, where $r(\mathbf{F}_m^{(i)}) = l$ implies that the observation was assigned to the lth component ($l = 1, \ldots, g_i$). The optimal or Bayes rule $r_B(\mathbf{F}_m^{(i)})$ for the allocation of $\mathbf{F}_m^{(i)}$ is defined by

$$r_B\left(\mathbf{F}_m^{(i)}\right) = l, \quad \text{if } \psi_l\left(\mathbf{F}_m^{(i)}\right) \geq \psi_h\left(\mathbf{F}_m^{(i)}\right), \quad h = 1, \ldots, g_i \tag{7}$$

where $\psi_l(\mathbf{F}_m^{(i)})$ is the posterior probability that the entity belonged to the lth component, with $\mathbf{F}_m^{(i)}$ having been observed on it, and it is given by

$$\psi_l\left(\mathbf{F}_m^{(i)}\right) = \text{pr}\left\{\text{entity} \in l\text{th component} | \mathbf{F}_m^{(i)}\right\}$$
$$= \frac{\pi_l \phi_l\left(F_m^{(i)}\right)}{\sum_{h=1}^{g} \pi_h \phi_h\left(F_m^{(i)}\right)}. \tag{8}$$

Relating the classes corresponding to the time variations of EMG signal characteristics to the g clusters was straightforward. Therefore, the set of classes for each muscle i could be redefined as $\mathbf{f}^{(i)} = \{f_1^{(i)}, f_2^{(i)}, \ldots, f_{g_i}^{(i)}\}$, where g_i is the number of components fitted to the data collected from muscle i.

Therefore, from the aforementioned analysis and after the training period, the class related to the recorded time-varying signals features was assigned to each muscle i at each time instance m using (5). Then, the decision for the global class f_G was made using the classes of all the muscles, $f_s^{(i)}$, $i = 1, \ldots, 9$, and by deciding which of the classes was most *popular* among the muscles. Let P_h be the sets that include the muscles whose assigned class is h, $h = 1, \ldots, g$. Thus, if Π is the union of the sets P_h, $h = 1, \ldots, g$, $\Pi = P_1 \bigcup P_2 \cdots \bigcup P_g$, we had $\overline{\overline{\Pi}} = 9$, where $\overline{\overline{\Pi}}$ is the total number of population of the sets, which coincided with the number of muscles. Then, we defined an allocation rule $r_B(f_G)$ for assigning the global class f_G to one of the possible classes, where $r_B(f_G) = f_l$ implies that the global class is assigned to the lth class ($l = 1, \ldots, g_i$). Therefore, the optimal rule for the allocation of f_G is defined by $r_B(f_G) = \arg\max_h \overline{\overline{P_h}}$, where $\overline{\overline{P_h}}$ is the population number of the set P_h, $h = 1, \ldots, g$. The aforementioned rule essentially means that the global class f_G was the one that coincided with the class assigned to the majority of the recorded muscles.

As noted before, the switching between the class assignments of the muscles was controlling the switching between the members of a set of decoding models. This resulted in a robust decoding method, the accuracy of which was not affected by the changes of EMG time-varying characteristics. The analysis of the switching decoder is presented in the next section.

C. Class-Dependent Switching Decoder

Since the number of muscles recorded was quite large (i.e., 9), a low-dimensional (low-D) representation of muscle activations was used instead of individual activations. This was based on the muscle synergies during motion of the arm, which have been discussed in the biomechanics literature [17]. The processed EMG recordings were represented into a low-D space, using the principal component analysis (PCA) algorithm [16]. It was found that a 2-D space could most represent the original high-dimensional data variance (i.e., more than 96%). The authors had used the dimensionality reduction for muscle activations in the past for planar movements of the arm [18]. Therefore, the details of the method application are omitted. Furthermore, the dimensionality reduction technique was also used for representing the arm motion in a low-D space, revealing motion primitives that are extensively discussed in the literature [19]. Therefore, by using the PCA algorithm, the analyzed 4-DOF motion, described in joint space (i.e., q_1, q_2, q_3, q_4), was represented into a low-D space. Specifically, it was found that most of the original data variance (i.e., 97%) was represented using a 2-D space. The next step was to build a model that will use the EMG low-D embeddings to estimate performed motion. It is quite obvious that from a physiological point of view, a model that would describe the function of the skeletal muscles in actuating the human joints would be generally a complex one. Using such a model for real-time decoding would be problematic. For this reason, we adopted a more flexible decoding model in which we introduced "hidden," or "latent" variables that we called $\mathbf{x}$. These hidden variables could model the unobserved, intrinsic system states, and thus, facilitated the correlation between the low-D embeddings for the muscles activation $\mathbf{U}$ and joint angles $\mathbf{y}$. Let $\mathbf{U}_t \in \mathbb{R}^2$ be the 2-D vector of the low-D representation of the nine muscle recordings at time $t = kT, \quad k = 1, \ldots$. Let $\mathbf{y}_t \in R^2$ be the low-D embedding of the arm joint angles at the same time instance. The model that was used for decoding the EMG activity to performed motion was defined by

$$\mathbf{x}_{t+1} = \mathbf{A}\mathbf{x}_t + \mathbf{B}\mathbf{U}_t + \mathbf{v}_t$$
$$\mathbf{y}_t = \mathbf{C}\mathbf{x}_t + \upsilon_t \qquad (9)$$

where $\mathbf{x}_t \in \mathbb{R}^d$ is a hidden state vector, d the dimension of this vector, and $\mathbf{v}_t$ and υ_t are zero-mean Gaussian noise variables in the process and observation equations, respectively, i.e., $\mathbf{v}_t \sim N(\mathbf{0}, \mathbf{W})$, $\upsilon_t \sim N(\mathbf{0}, \mathbf{Q})$, where $\mathbf{W} \in \mathbb{R}^d$ and $\mathbf{Q} \in \mathbb{R}^2$ are the covariance matrices of $\mathbf{v}_t$ and υ_t, respectively. Details on the model structure can be found in [18].

A distinct model described by (9) was used for each of the g possible global classes. During the training phase, after defining the class of each muscle using (8), the global class f_G was defined. Then, each of the g models of the form (9) was trained

using the low-D embeddings of the muscle recordings and the corresponding joint angles. Data belonging to each one of the possible global classes were used only for the corresponding decoding model. Model fitting was defined by the estimation of the following parameters: matrices $\mathbf{A}$, $\mathbf{B}$, and $\mathbf{C}$, and noise covariance matrices $\mathbf{W}$ and $\mathbf{Q}$. Given a training set, the model parameters could be found using an iterative prediction-error-minimization (i.e., maximum likelihood) algorithm [20].

During real-time operation, the g trained models were used to transform the low-D embeddings of muscle activations to low-D embeddings of joint angles. Then, using the transformation defined by the PCA algorithm, the high-dimensional representation of the arm motion (four joint angles) were computed (see [18] for details).

D. Robot Control

A 7-DOF anthropomorphic robot arm (PA-10, Mitsubishi Heavy Industries) was used. Only 4 DOFs of the robot were actuated (joints of the shoulder and elbow), while the others were kept fixed at zero position via electromechanical brakes. The arm was horizontally mounted to mimic the human arm. The robot motors were controlled in torque. In order to control the robot arm using the desired joint angle vector $\mathbf{q_d}$,[2] an inverse dynamic controller was used, which is defined by

$$\tau = \mathbf{I}(\mathbf{q_r})(\ddot{\mathbf{q}}_d + \mathbf{K_v}\dot{\mathbf{e}} + \mathbf{K_p}\mathbf{e}) + \mathbf{G}(\mathbf{q_r})$$
$$+ \mathbf{C}(\mathbf{q_r}, \dot{\mathbf{q}}_r)\dot{\mathbf{q}}_r + \mathbf{F_{fr}}(\dot{\mathbf{q}}_r) \qquad (10)$$

where $\tau = [\tau_1 \quad \tau_2 \quad \tau_3 \quad \tau_4]^T$ is the vector of robot joint torques, $\mathbf{q_r} = [q_{1r} \quad q_{2r} \quad q_{3r} \quad q_{4r}]^T$ are the robot joint angles, $\mathbf{K_v}$ and $\mathbf{K_p}$ are gain matrices, and $\mathbf{e}$ is the error vector between the desired and the robot joint angles, i.e.

$$\mathbf{e} = [q_{1d} - q_{1r} \quad q_{2d} - q_{2r} \quad q_{3d} - q_{3r} \quad q_{4d} - q_{4r}]^T. \qquad (11)$$

Further, $\mathbf{I}$, $\mathbf{G}$, $\mathbf{C}$, and $\mathbf{F_{fr}}$ are the inertia tensor, the gravity vector, the Coriolis–centrifugal matrix, and the joint friction vector of the four actuated robot links and joints, respectively, identified in [21]. By using the aforementioned controller, the robot arm was teleoperated by the user in real time, using the proposed methodology for decoding user's arm motion from EMG signals.

III. RESULTS

A. Experimental and Verification Procedures

The proposed architecture was assessed through remote teleoperation of the robot arm using only EMG signals from the nine muscles, as analyzed before. The robot arm used was a 7-DOF anthropomorphic manipulator (PA-10, Mitsubishi Heavy Industries). Details of the setup can be found in [18].

The system training phase had no resting periods. The duration of the training phase was decided to be 4 min, since after that period, the user wanted to rest his/her arm. Moreover, during the real-time operation, a possible user would not be able to teleoperate the robot arm in the 3-D space for more than 4 min

---

[2]The vector of joint angles is decoded from EMG signals.

without a resting period. As soon as the training period ended and the proposed switching model was trained, the real-time operation phase commenced. During this phase, the user had visual contact with the robot arm, while teleoperating it in the 3-D space. Only EMG signals were used for estimating arm motion, and finally, controlling the robot arm in real time. The position tracking system was kept into place for a few experiments, only for offline validation purposes. Five experimental sessions were conducted using each subject, with each session lasting for 3.5 min. Real and estimated motion data were recorded during these sessions for evaluating the models' performance. The real joint angle profiles were computed from the position tracker sensors, which were kept in place (i.e., on the user's arm) for offline validation purpose. Using the kinematic equations, we computed the estimated hand trajectory in the 3-D space using the estimated joint angles. This phase could have as many resting periods as desired by the user; however, it was noticed that usually the user was resting his/her arm after approximately 3 min of operation. The system was tested by four able-bodied persons, who found it convenient and accurate while they were easily acquainted with its operation. All experimental procedures were conducted under a protocol approved by the National Technical University of Athens' Institutional Review Board.

The proposed methodology was compared with other models used in the literature for decoding a continuous representation of motion using EMG signals. The linear filter method, widely used in the literature for decoding motion using neural signals, was used. The support vector machines (SVMs) method was also used [4]. The experimental data used for model comparison were the same within the models and were collected through experimental sessions in which four male subjects (age group: 24–30 years) participated. The criterion that was used for assessing the accuracy of the reconstruction of human motion using the decoding models was the correlation coefficient (CC). The latter essentially describes the similarity between the reconstructed and the true motion profiles and constitutes the most common means of reconstruction assessment for decoding purposes. Perfect matching between the estimated and the true angles corresponds to CC = 1.

B. Methodology Assessment Results

The estimated user's hand 3-D trajectory, along with the ground truth for an experimental session with one of the subjects, is depicted in Fig. 4(a). As can be seen, the method could estimate the hand trajectory with high accuracy, compensating for EMG changes with respect to time. The latter is shown in Fig. 4(a), where the estimates based on a stationary decoding model of the same form of (9), which did not compensate for EMG time variation, are shown. As can be seen, using a stationary model, the accuracy of the estimates decreases with time, due to time variation of EMG signals. Table I includes the mean values and standard deviation values of CC for the 3-D hand trajectory estimates coming from the switching model, the stationary model, and the other two methods used, i.e., the linear filter and the SVM algorithm. Data from five experimental sessions, each lasting 3.5 min, across all the four subjects par-
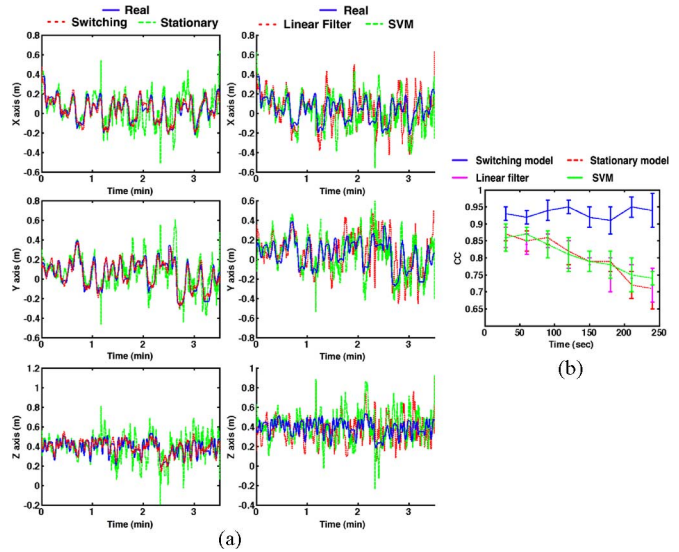

Fig. 4. (a) Real and estimated hand trajectory along the x-, y-, and z-axis, for a 3.5-min period. Estimates from the proposed switching method are found to be quite close to the ground truth during the whole 3.5-min test, while the other models' accuracy decreases after a period of approximately 60 s. (b) CC values (mean and standard deviations) for the estimated user's hand position in the Cartesian space with respect to time, using the four models. Real and estimated distances of the user's hand with respect the origin of the Cartesian reference system was used for computing the criteria values.

TABLE I
EFFECTIVENESS COMPARISON AMONG DIFFERENT DECODING METHODS

Decoding model	CC_x	CC_y	CC_z
Switching model	0.93 ± 0.02	0.94 ± 0.02	0.93 ± 0.03
Stationary model	0.84 ± 0.03	0.81 ± 0.02	0.81 ± 0.03
Linear Filter	0.81 ± 0.05	0.82 ± 0.04	0.81 ± 0.05
SVM	0.82 ± 0.03	0.84 ± 0.02	0.82 ± 0.05

ticipated were used. As can be seen, the proposed model was highly accurate in predicting arm motion, and it outperformed the other methods.

The accuracy of the four compared methods in estimating arm motion with respect to time is shown in Fig. 4(b). The CC values for the Cartesian position of the user's hand in the 3-D space were calculated at each time interval of 30 s.[3] Data only within the corresponding 30-s interval were used. Mean and standard deviation values were calculated for the five experimental sessions, across the four subjects who participated. As can be seen, the proposed model was able to robustly estimate user's motion, while the other three models showed deteriorating accuracy with respect to time.

IV. CONCLUSION

In this paper, a methodology for controlling an anthropomorphic robot arm using EMG signals from the muscles of the upper limb was proposed. EMG signals recorded from muscles of the upper limb were used for extracting kinematic variables (i.e.,

---

[3]The distance of the user's hand with respect to the origin of the Cartesian reference system was used, instead of each coordinate separately, for simplicity.

joint angles) in order to control an anthropomorphic robot arm in real time. EMG signal characteristics changes are usually noticed after a period of approximately 30 s of operation [10]. For this reason, a probabilistic framework was designed in order to assign to each of the muscles recorded a *class* related to the recorded time-varying signal features. Then, a switching model was built in such a way that it compensated for the EMG changes. From the experiments with four subjects, it was shown that the proposed method could estimate the human arm motion using only EMG signals with high accuracy.

The novelty of the method proposed here can be centered around two main issues. First, the proposed method is not affected by EMG changes with respect to time. Since EMG is widely known as a nonstationary signal, the fact that the proposed method can compensate for EMG changes through time (caused by muscle fatigue or changes in the level of muscle force production) is quite important for the field. The second important issue presented here is that, to the best of our knowledge, this was the first time a continuous profile of 3-D arm motion (including 4 DOFs) was extracted using only EMG signals. Moreover, this study proposes a methodology that can be easily trained to each user and takes little time to build the decoding model, while the computational load during real-time operation is negligible.

REFERENCES

[1] J. Park and O. Khatib, "A haptic teleoperation approach based on contact force control," *Int. J. Robot. Res.*, vol. 25, no. 5/6, pp. 575–591, 2006.

[2] F. E. Zajac, "Muscle and tendon: Properties, models, scaling, and application to biomechanics and motor control," *CRC Crit. Rev. Biomed. Eng.*, vol. 17, pp. 359–411, 1986.

[3] O. Fukuda, T. Tsuji, M. Kaneko, and A. Otsuka, "A human-assisting manipulator teleoperated by EMG signals and arm motions," *IEEE Trans. Robot. Autom.*, vol. 19, no. 2, pp. 210–222, Apr. 2003.

[4] S. Bitzer and P. van der Smagt, "Learning EMG control of a robotic hand: Towards active prostheses," in *Proc. IEEE Int. Conf. Robot. Autom.*, 2006, pp. 2819–2823.

[5] K. Kiguchi, S. Kariya, K. Watanabe, K. Izumi, and T. Fukuda, "An exoskeletal robot for human elbow motion support—Sensor fusion, adaptation, and control," *IEEE Trans. Syst., Man, Cybern. B, Cybern.*, vol. 31, no. 3, pp. 353–361, Jun. 2001.

[6] K. Kita, R. Kato, H. Yokoi, and T. Arai, "Development of autonomous assistive devices—Analysis of change of human motion patterns," in *Proc. IEEE Int. Conf. Syst., Cybern.*, 2006, pp. 316–321.

[7] A. V. Hill, "The heat of shortening and the dynamic constants of muscle," *Proc. R. Soc. Lond. Biol.*, vol. 126, pp. 136–195, 1938.

[8] E. Cavallaro, J. Rosen, J. C. Perry, S. Burns, and B. Hannaford, "Hill-based model as a myoprocessor for a neural controlled powered exoskeleton arm parameters optimization," in *Proc. IEEE Int. Conf. Robot. Autom.*, 2005, pp. 4514–4519.

[9] P. K. Artemiadis and K. J. Kyriakopoulos, "Teleoperation of a robot manipulator using EMG signals and a position tracker," in *Proc. IEEE/RSJ Int. Conf. Intell. Robots Syst.*, 2005, pp. 1003–1008.

[10] N. A. Dimitrova and G. V. Dimitrov, "Interpretation of EMG changes with fatigue: Facts, pitfalls, and fallacies," *J. Electromyogr. Kinesiol.*, vol. 13, pp. 13–36, 2003.

[11] P. K. Artemiadis and K. J. Kyriakopoulos, "Assessment of muscle fatigue using a probabilistic framework for an EMG-based robot control scenario," in *Proc. IEEE Int. Conf. Bioinf. Bioeng.*, 2008, pp. 1–6.

[12] M. M. Morlock, V. Bonin, G. Muller, and E. Schneider, "Trunk muscle fatigue and associated EMG changes during a dynamic iso-inertial test," *Eur. J. Appl. Physiol.*, vol. 76, pp. 75–80, 1997.

[13] D. M. Mirkov, S. Milanovic, D. B. Ilic, and S. Jaric, "Symmetry of discrete and oscillatory elbow movements: Does it depend on torque that the agonist and antagonist muscle can exert?," *Motor Control*, vol. 6, pp. 271–281, 2002.

[14] J. R. Cram and G. S. Kasman, *Introduction to Surface Electromyography*. Gaithersburg, MD: Aspen, 1998.

[15] J. Jeong, W. Cho, Y. Kim, and H. Choi, "Recognition of lower limb muscle EMG patterns by using neural networks during the postural balance control," in *Proc. Int. Conf. Biomed. Eng. 2006*, 2007, pp. 82–85.

[16] G. McLachlan and D. Peel, *Finite Mixture Models*. New York: Wiley, 2000.

[17] A. d'Avella, A. Portone, L. Fernandez, and F. Lacquaniti, "Control of fast-reaching movements by muscle synergy combinations," *J. Neurosci.*, vol. 25, no. 30, pp. 7791–7810, 2006.

[18] P. K. Artemiadis and K. J. Kyriakopoulos, "EMG-based teleoperation of a robot arm using low-dimensional representation," in *Proc. IEEE/RSJ Int. Conf. Intell. Robots Syst.*, 2007, pp. 489–495.

[19] B. Lim, S. Ra, and F. Park, "Movement primitives, principal component analysis, and the efficient generation of natural motions," in *Proc. IEEE Int. Conf. Robot. Autom.*, 2005, pp. 4630–4635.

[20] L. Ljung, *System Identification: Theory for the User*. Upper Saddle River, NJ: Prentice-Hall, 1999.

[21] N. A. Mpompos, P. K. Artemiadis, A. S. Oikonomopoulos, and K. J. Kyriakopoulos, "Modeling, full identification and control of the mitsubishi PA-10 robot arm," in *Proc. IEEE/ASME Int. Conf. Adv. Intell. Mechatronics*, Switzerland, 2007, pp. 1–6.

Panagiotis K. Artemiadis (M'07) received the Diploma and the Ph.D. degree in mechanical engineering from the National Technical University of Athens, Athens, Greece, in 2003 and 2009, respectively.

Since 2009, he has been a Postdoctoral Associate in the Newman Laboratory for Biomechanics and Human Rehabilitation, Department of Mechanical Engineering, Massachusetts Institute of Technology, Cambridge. His current research interests include the area of rehabilitation robotics, neurorobotics, control of robot manipulator, and mechatronics. He has authored or coauthored more than 17 papers published in journals and presented at refereed conferences, and three of them have been included in the top papers in international conferences. He has been a Reviewer and an Associate Editor of a number of journals and conferences, and has worked on projects funded by the European Commission.

Dr. Artemiadis is a member of the Hellenic Bioscientific Association and the Technical Chamber of Greece.

Kostas J. Kyriakopoulos (S'86–M'90) received the Diploma (with honors) in mechanical engineering from the National Technical University of Athens (NTUA), Athens, Greece, in 1985, and the M.S. and Ph.D. degrees in electrical, computer, and systems engineering (ECSE) from Rensselaer Polytechnic Institute (RPI), Troy, NY, in 1987 and 1991, respectively.

From 1988 to 1991, he was with the Center for Intelligent Robotic Systems for Space Exploration, National Aeronautics and Space Administration. During 1991–1993, he was an Assistant Professor of ECSE at RPI and also at the New York State Center for Advanced Technology in Automation and Robotics. Since 1994, he has been with the Control Systems Laboratory, School of Mechanical Engineering, NTUA, where he is currently a Professor and the Director of the Departmental Computation Laboratory. His current research interests include the area of nonlinear control systems applications in sensor-based motion planning and control of multirobotic systems: manipulators and vehicles (mobile, underwater, and aerial) and micro- and biomechatronics. He has authored or coauthored approximately 180 papers published in journals and presented at refereed conferences. He is a member of the editorial committees of a number of journals.

Prof. Kyriakopoulos is a member of the European Robotics Research Network and the Technical Chamber of Greece. He was awarded the G. Samaras Award of Academic Excellence by the NTUA, the Bodosakis Foundation Fellowship (1986–1989), the Alexander Onassis Foundation Fellowship (1989–1990), and the Alexander Von Humboldt Foundation Fellowship (1993). He has been an administrative member of a number of international conferences.